Studies on Novel Nanosuperabsorbent Composites: Swelling Behavior in Different Environments and Effect on Water Absorption and Retention Properties of Sandy Loam Soil and Soil-less Medium

Anupama Singh,[1] Dhruba Jyoti Sarkar,[1] Anil Kumar Singh,[2] Rajender Parsad,[3] Anil Kumar,[3] Balraj Singh Parmar[1]

[1]*Division of Agricultural Chemicals, Indian Agricultural Research Institute, New Delhi, India*
[2]*Indian Council of Agricultural Research, New Delhi, India*
[3]*Indian Agricultural Statistics Research Institute, New Delhi, India*

Received 8 January 2010; accepted 15 August 2010
DOI 10.1002/app.33263

ABSTRACT: A novel nanosuperabsorbent composite (NSAPC) was prepared by *in situ* grafting polymerization and cross-linking on to a novel biopolymer of plant origin (complex heteropolysaccharide in nature) in the presence of a clay mineral using a green chemistry technique. The optimization studies of various synthesis parameters, namely, type of clay, backbone/clay ratio, monomer concentration, cross-linker concentration, initiator concentration, quantity of water per unit reaction mass, particle size of backbone, etc., were done. The NSAPC was characterized by X-ray diffraction and scanning electron microscopy. Swelling behavior of NSAPC in response to external stimuli namely salt solutions, fertilizer solutions, temperature, and pH was studied and compared with the performance of P-gel, a commercial superabsorbent material developed earlier in our laboratory. The NSAPC exhibited significant swelling in various environments. Effect of NSAPC on water absorption and retention characteristics of sandy loam soil and soil-less medium was also studied as a function of temperature and tensions. Addition of NSAPC significantly improved the moisture characteristics of plant growth media (both soil and soil-less), showing that it has tremendous potential for diverse applications in moisture stress agriculture. © 2010 Wiley Periodicals, Inc. J Appl Polym Sci 120: 1448–1458, 2011

Key words: biopolymers; composites; swelling; clay

INTRODUCTION

In view of the fast depletion of ground water reserves, uncertainty of rains in arid and semiarid regions of the world, coupled with the growing food demands of the burgeoning human population, efficient use of water available for crops has become highly relevant. In recent years, the use of superabsorbent polymers (SAPs) has been viewed as an innovative tool to improve water use efficiency in agricultural operations. Since the report of the first SAP by United States Department of Agriculture,[1] the research on developing better products for use in agriculture continues world wide. Polymeric soil conditioners have been known since 1950s.[2] These polymers were developed to improve the physical properties of soil such as water-holding capacity (WHC), soil permeability, and infiltration rates, facilitating plant development, especially in structureless soils in areas subject to drought.[2–5] In addition, purely synthetic as well as semisynthetic hydrogels have been used for removal of heavy metals from water as well as controlled release agro-input devices in agriculture.[6–11]

However, the effects of hydrogel technology in agriculture are inconclusive because contradictory effects on physical properties of growing media have been reported.[12–25] Although a number of commercial hydrogels have been tried and recommended in agriculture and horticulture, their use on a large scale remains limited primarily because of high cost, high rate of application, and their inability to perform under harsh agro-climatic conditions.[26,27] To overcome the impediments of the harsh conditions of tropical soils, a SAP of semisynthetic origin "Pusa-gel" has been developed and commercialized from our laboratory (indicated as P-gel in this study). Pusa-gel is a cross-linked superabsorber obtained by a process involving grafting and cross-linking acrylate onto cellulosic backbone (backbone-monomer ratio: 1 : 0.75 on % weight basis).[28] The nanocomposite studied in this work was developed to explore the possibility of a better alternative to P-gel.

Correspondence to: A. Singh (anupama.chikara@gmail.com).

Journal of Applied Polymer Science, Vol. 120, 1448–1458 (2011)

Superabsorbent composites and nanocomposites have been receiving great attention in recent years because of their unusual and enhanced properties over conventional hydrogels.[29] Bionanocomposites add a new dimension to these enhancements because of their ecofriendly and biocompatibility characteristics.[30] Utility of this new class of hybrid materials in biomedical applications such as tissue engineering, bone reconstruction, etc. has already been established.[31,32] However, little or no research on their behavior in plant growth environments has been reported. A critical factor underlying the application scope of bionanocomposite properties is interaction between chosen matrix and the filler. In view of this, a series of novel polyacrylate/biopolymer clay-intercalated nanocomposites was synthesized by a novel process and characterized.[33] The biopolymer chosen was a plant-based (*Cochlospermum* sps.) complex heteropolysaccharide containing galactose, rhamnose, and galacturonic acid units. A distinct character of this biopolymer is its ability to retain water (80 g/g, w/w basis).

In this article, the effect of various synthesis parameters on the water absorbency of novel composites has been reported and supported by structural characterization. In the second part of this study, the comparative evaluation of optimized nanocomposite [nanosuperabsorbent composite (NSAPC), backbone-monomer ratio: 1 : 2 on % weight basis] and P-gel in different salt and fertilizer solutions as well as their effect on water absorption and retentive capacity of sandy loam soil and soil-less media has been presented.

EXPERIMENTAL

Materials

Commercial-grade amorphous resin (complex heteropolysaccharide derived from *Cochlospermum* species), dry micropowdered clays, acrylamide, *N*,*N*′-methylenebisacrylamide cross-linker, and a persulfate initiator were purchased locally and used as received without further purification.

Preparation of nanocomposites

The NSAPC were prepared by *in situ* grafting polymerization of acrylamide on the resin backbone in the presence of clay mineral and cross-linker using persulfate initiator in microwave-assisted free-radical polymerization technique.[33] To optimize the concentration of various synthesis parameters, a sequential completely randomized design was adopted. A typical procedure is as follows: An aqueous solution containing specific weight ratio of resin and clay, monomer, and cross-linker was heated upto 80°C for a period of few seconds, followed by addition of initiator. The mixture was kept as such for a couple of hours. The resulting product was washed with distilled water and air dried under ambient conditions. The dehydrated sample was further vacuum dried till constant weight. The dried product was milled and screened through 300-mesh-size screen.

Wide-angle X-ray diffraction (XRD) measurements were performed using a Philips PW1710 diffractometer control equipped with Philips PW1728 X-ray generator. The scanning range was 3–20° 2θ, with a scanning rate of 1.2° 2θ/min. Scanning electron microscopy images were obtained with a Zeiss EVO Series scanning electron microscope (EVO 50) with resolution of 2.0 nm at 30 kV.

Water absorbency measurements

A composite sample weighing 0.1 g (particle size 100–240 mesh size) was immersed in the excess of distilled water (pH 7.0, EC 0.001 mhos/cm) in triplicate and kept at two temperatures, 25°C and 45°C, separately until equilibrium was attained. Free water was filtered through a nylon sieve (200 mesh size), gel allowed to drain on sieve for 10 min, and finally weighed. The water absorbency (Q_{H_2O}) was calculated using the following equation:

$$Q_{H_2O}\ (g/g) = (w_2 - w_1)/w_1,$$

where w_1 is the weight of xerogel (dry absorbent) and w_2 is the weight of swollen gel. Q_{H_2O} was calculated as grams of water per gram of dry sample. The NSAPC exhibiting maximum absorption in distilled water was further evaluated and compared with P-gel in different salt solutions.

Salt solution absorbency measurements

Dry P-gel and NSAPC were milled separately to achieve particle size in the range (100–240 mesh size). Aqueous solutions of different strengths (5, 10, 15, and 20 m*M*) of four salts namely ammonium sulfate (AS), ammonium nitrate (AN), potassium nitrate (PN), sodium chloride (SC), and one fertilizer namely urea (U) were prepared and used. The dried and milled sample was immersed in salt solution of a particular strength at 25°C. The swollen gel was weighed after 24 h, using same equation as above.

Similar experiment was repeated in tap water (pH 7.87, EC 1.099 mhos/cm), hard water, and aqueous solutions of pH 4, 7, and 9. Hard waters of three different strengths were prepared in the laboratory according to CIPAC standard method and labeled as hard water A (hardness 20 ppm, pH 5–6, and Ca : Mg ratio 50 : 50), hard water B (hardness 20 ppm, pH 8–9,

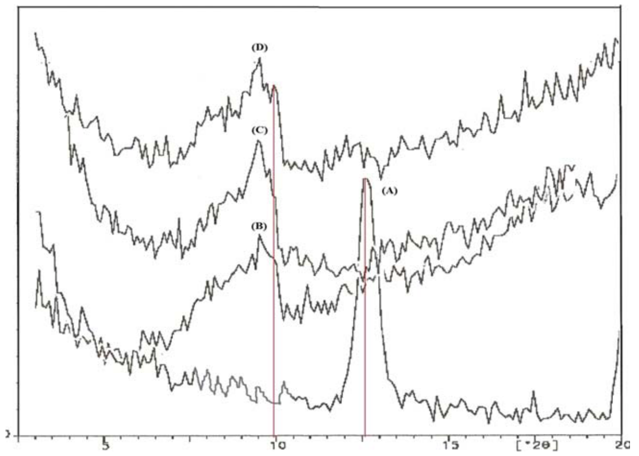

Figure 1 XRD patterns of clay (A), backbone (B), NSAPC (C), and clay-free gel (D). [Color figure can be viewed in the online issue, which is available at wileyonlinelibrary.com.]

and Ca : Mg ratio 80 : 20), and hard water C (hardness 500 ppm, pH 7–8, and Ca : Mg ratio 80 : 20).

Water absorption and retention measurement in soil and soil-less media

Sandy loam soil and soil-less media (a sterilized mixture of cocopeat, vermiculite, and perlite in the ratio 3 : 1 : 1 on volume basis) were collected from institute farm and protected cultivation nursery, respectively. Air-dried soil sample was passed though the 2-mm sieve and mixed with P-gel and NSAPC at the rate of 0.5% and 0.75% each. Soil-less medium was dried till constant weight was attained and used as such.

For water absorption, desired amounts of amended soil (50 g) or soil-less medium (20 g) were taken in preweighed plastic cups having perforated bases fitted with filter papers. Subsequently, each cup was immersed overnight in water to saturate through capillary water rise. Water held by the sample was determined gravimetrically. WHC of soil and soil-less medium was calculated by the following equation:

$$\mathrm{WHC}\ (\%) = M - m/m \times 100,$$

where M denotes weight of wet sample (g) and m denotes weight of oven-dried sample (g).

Water retention study was done using pressure plate apparatus at different tensions: 2pF, 2.4pF, 2.7pF, 3pF, 3.7pF, and 4.2pF. Ceramic plates were kept overnight in water for saturation. Amended soil and soil-less media were filled in rubber rings arranged on bar plates and allowed to saturate overnight. Care was taken to ensure proper contact between the samples and ceramic plate surface. The saturated samples along with ceramic plates were placed in pressure chamber pertaining to different tensions. The pressure was applied and maintained till water stopped flowing out of the chamber. Samples were transferred to moisture boxes immediately and weighed. The moist samples were dried in a hot air oven at 105°C for 24 h, air cooled, and reweighed. The amount of water held at particular pressure was calculated using following equation:

$$\mathrm{WC}\ (\%\ \text{by weight}) = (W_{\mathrm{wet}} - W_{\mathrm{dry}}/W_{\mathrm{dry}}) \times 100$$

where WC is the percent water content of soil or soil-less media on weight basis, W_{wet} is the mass of wet soil or soil-less media at a particular tension, and W_{dry} is the weight of oven-dried soil or soil-less medium.

Statistical analysis

The experiments on effect of various parameters on water absorbency values were conducted using factorial completely randomized design. To identify the best treatment combinations, the data were analyzed by one-way classified analysis using PROC GLM procedure of SAS package (SAS Institute, Cary, NC).

RESULTS AND DISCUSSION

Identification of superabsorbent nanocomposite

The XRD patterns of clay (1 : 1 type) (A), back bone (B), NSAPC(C), and clay-free gel (D) are shown in Figure 1. The values of interlayer spacing in A, B, C, and D (Table I) were calculated using Bragg's law ($n\lambda = 2d \sin\theta$). The scattering curve of clay (A) shows a prominent XRD peak because of layered crystalline structure corresponding to c-axis spacing at 7.016 E ($2\theta = 12.6°$). The backbone (B) exhibited a distinguishable peak indicating its ordered structural configuration corresponding to spacing at 9.29 Å ($2\theta = 9.5°$). The same peak is retained in the scattering curves of NSAPC(C) and clay-free gel (D). In the XRD pattern of NSAPC, in which clay was incorporated during polymerization, the peak corresponding to A at 7.016 Å disappeared, with simultaneous appearance of a peak, at $2\theta = 10°$; c-axis spacing was 8.98 Å. The significant difference in the peak positions corresponding to clay established that the

TABLE I
Interlayer Spacing Values of in Clay (A), Backbone (B), Nanocomposite (C), and Clay-Free Gel (D)

Material	Spacing (Å)
A	7.016
B	9.29
C	8.98, 9.29
D	9.29

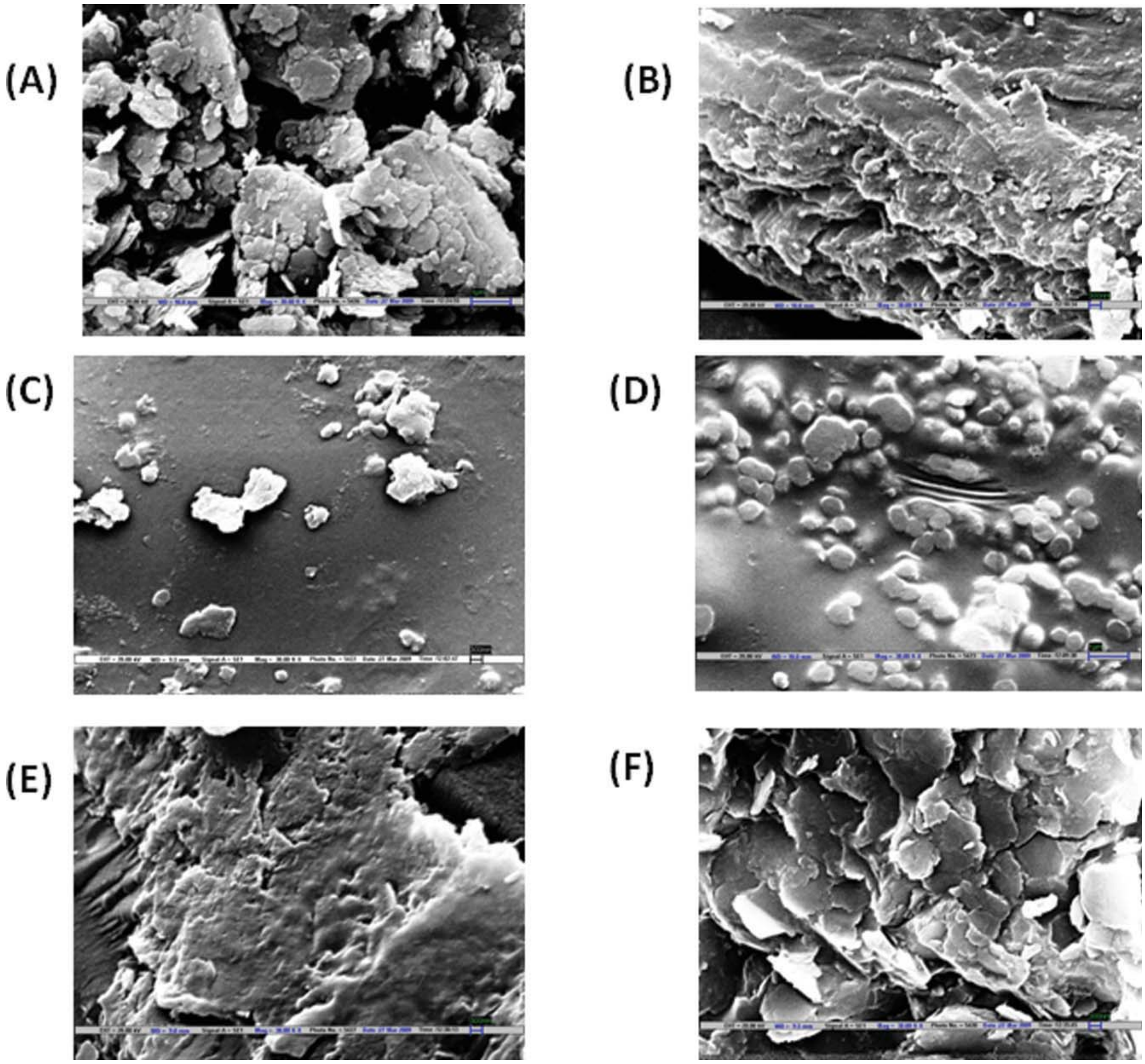

Figure 2 Scanning electron micrographs (×30,000K) for clay (A), backbone (B), clay-free gel (C), and composites of various backbone clay ratios (D, E, and F). [Color figure can be viewed in the online issue, which is available at wileyonlinelibrary.com.]

NSAPC, prepared by *in situ* solution polymerization process, was an intercalated nanocomposite.

Surface morphology of nanocomposites under scanning electron microscope was examined to investigate arrangement of clay aggregates in the matrix of the polymers. Figure 2 compares microscopic surfaces of clay A, backbone B, clay-free gel C, and composites D, E, and F with backbone/clay ratios 1/0.1, 1/0.3, and 1/1, respectively. Micrograph of clay exhibited disordered flakes with ragged and somewhat irregular edges, indicating that the clay mineral used in the composite synthesis was poorly crystalline. This observation is in conformity with observation reported in Grim.[34] Micrograph of backbone (B) revealed a well-defined layer of polysaccharide unites of varying lengths. Comparison of morphology of clay-free gel with the composites showed nearly smooth surface of clay-free gel because of homogenous grafting and cross-linking of monomer onto the backbone, whereas the composites, particularly those containing higher clay proportions (E and F), displayed fractured but specific topography, because of orientation of layered clay particles into the matrix of backbone. Absence of any nonhomogenous scattering of clay aggregates was an indication of a good degree of its participation in the polymerization reaction leading to composite formation. This fact was further substantiated by the presence of hydrophilic polar groups in the lattice of clay, which seemed to have taken part in the reaction process.

TABLE II
Effect of Clay Type *vis-a-vis* Monomer Content on Water Absorbency

Clay Type	Monomer (wt %)	% Add-on	Q_{H_2O} (g/g) 25°C	Q_{H_2O} (g/g) 45°C
Clay-1	32.96	36.00	72.17^{m}	82.16^{l}
	39.60	74.00	83.64^{l}	$85.48^{l,k}$
	56.73	216.00	$95.10^{j,i}$	$108.10^{h,g}$
	66.29	351.00	$114.52^{f,g}$	$121.00^{e,f}$
Clay-2	32.96	53.00	68.03^{n}	$108.90^{h,g}$
	39.60	112.00	126.19^{e}	168.93^{b}
	56.73	205.00	174.08^{b}	211.20^{a}
	66.29	146.00	$109.53^{h,g}$	171.00^{b}
Clay-3	32.96	03.00	$89.85^{j,l,k}$	97.87^{i}
	39.60	35.00	142.43^{d}	160.13^{c}
	56.73	135.00	124.07^{e}	$93.67^{j,i}$
	66.29	306.00	$108.70^{h,g}$	75.63^{m}
Clay-4	32.96	24.00	$95.60^{j,i}$	124.23^{e}
	39.60	77.00	$95.63^{j,i}$	128.06^{e}
	56.73	200.00	$121.13^{e,.f}$	159.03^{c}
	66.29	368.00	106.40^{h}	$109.03^{h,g}$

Backbone : clay ratio, 1 : 0.5; backbone : cross-linker ratio, 1 : 0.025.

Least significant difference at 5%: 7.48; Means within columns followed by different superscript letters are significantly different at 5% level of significance and those followed by the same letter does not differ significantly at 5% level of significance.

Effect of clay type *vis-à-vis* monomer concentration on water absorbency

The absorption values for superabsorbent composites prepared by variation of monomer concentration with four types of clay are shown in Table II. The samples containing clay-2 (1 : 1 type) exhibited maximum water absorption at 45°C. Remaining three clays, all belonging to 2 : 1 type, showed lesser swelling particularly at 45°C. In clay-1 series, increase in monomer concentration led to increase in water absorbency by the sample. In clay-2 series, the water absorbency increased with increase in monomer content from 32.96% to 56.73%. Further increase led to decrease in swelling. Clay-4 series also showed the similar trend. In clay-3 series, increase in swelling occurred up to 39.60% monomer content in the feed after which it decreased significantly. The clay-specific initial increase in water absorbency could be due to different extents of grafting (Table II). Decrease after a particular monomer concentration could be attributed to increase in homopolymer percentage, resulting in increase in soluble fraction at fixed cross-linking density.[35] However, in this study, because increase in monomer concentration has led to consistent increase in % add-on in all the series, the decrease in swelling after a particular monomer concentration may be explained in terms of phenomenon of self cross-linking as a result of grafting of higher amount of monomer, thus preventing accessibility of more solvent in the matrix.[6]

As regards the effect of clay type on water absorbency, the clay type is an important factor because composite formation involves copolymerization reaction between -OH groups of clay and polar functional groups of backbone and the vinyl monomer. Clays 1, 3, and 4 belong to the smectite group (2 : 1 type), which possess remarkably higher swelling ability on exposure to water compared with clay-2, which belongs to the kaolinite group (1 : 1 type). According to Table II, the Q_{H_2O} of the composite of clay-2 was higher than that of clays 1, 3, and 4. Because clays 1, 3, and 4 are more hydrophilic in nature than clay-2, their hydration and distension in reaction medium is more than in clay-1, which ultimately leads to higher cross-linking density in their composites. Higher cross-linking density leads to lower Q_{H_2O} values by not providing enough space for water entry and consequent swelling. This trend was similar to the one reported by Wu et al.[36]

Effect of clay content on water absorbency in deionized water

Water absorbency of nanocomposites in deionized water as a function of the clay content is shown in Table III. Water absorbency increased although nonsignificantly, with increasing weight percentage of clay-2. According to Flory's swelling theory,[37] water absorbency of a gel is directly proportional to the affinity of gel toward water, which in this study was maximum at or below 3 wt %. At molar ratios >3 wt %, water uptake decreased. This observation is in agreement with reports by Chen and Zhao,[38] who reported that the inorganic clay mineral acts as additional network point, resulting in increase in cross-linking with increase in clay content, manifesting in decreased water absorbency.

TABLE III
Effect of Clay-2 Content on the Water Absorbencies of Nanocomposites

Clay percentage (wt %)	Q_{H_2O} (g/g)	
	25°C	45°C
0.0	168.3^{a}	171.23^{a}
3.0	170.50^{a}	172.32^{a}
9.0	145.90^{b}	146.10^{b}
15.0	138.10^{c}	140.33^{c}
18.0	102.30^{e}	119.93^{d}
24.0	89.77^{f}	98.70^{e}

Synthesis parameters: weight ratio of monomer, cross-linker, and initiator to backbone, 2 : 1, 0.025 : 1, and 0.04 : 1, respectively.

Least significant difference at 5%: 5.32; Means within columns followed by different letters are significantly different at 5% level of significance and those followed by the same letter do not differ significantly at 5% level of significance.

Effect of cross-linker content on water absorbency

The effect of cross-linker content on water absorbency behavior of composites is shown in Table IV. The results indicate that the swelling ratio increased significantly with cross-linker concentration in the range 0.06–0.12 wt %, beyond which it significantly decreased with further increase in cross-linker concentration. The initial increase can be understood on the basis of the presence of hydrophilic groups in the molecular structure of cross-linker. Below 0.12 wt % of cross-linker, the soluble fraction remains more resulting in lesser absorbency of composite. Decreasing water uptake above 0.12 wt % can easily be explained in terms of generation of extensive cross-link points, resulting in highly cross-linked structures that cannot expand sufficiently to hold large quantities of water. This observation is supported by earlier reports.[39] At cross-linker content smaller than 0.006 wt %, the sample remains in sol–gel states in water and Q_{H_2O} cannot be determined.

Effect of volume of water in the feed on water absorbency

The variation of Q_{H_2O} with the volume of water in the feed, expressed as mL/g reaction mass is shown in Table III. It is clear that increase in quantity of water from 1.6% to 6.4% resulted in significant and exponential increase in Q_{H_2O} values. This could be due to increase in effective collisions between reactive moieties as the volume of water was increased upto 6.4%. Further increase led to inconsistent gel formation and increase in soluble fraction, which could be due to dilution of cross-linker, thus leading to poor network formation.

Effect of initiator concentration on water absorbency

The relationship between initiator concentration and the water absorbency is depicted in Table IV. Initial increase in initiator concentration upto 0.64 wt % led to increase in water uptake, beyond which further increase led to sharp reduction in swelling ratio. Initial increment in water absorbency could be attributed to rise in number of active radicals on the backbone. Subsequent decrease in absorbency can be explained in terms of the phenomenon of "self-cross-linking," a term cited by Chen and Zhao.[38] This refers to increase in terminating step reaction rate via bimolecular collisions, resulting in enhancement in cross-link density of the network.

TABLE IV
Effect of Cross-linker Content, Volume of Water Used, and Initiator on the Water Absorption Behavior of Nanocomposites at 25°C and 45°C

Cross-linker content[1] (wt %)	Q_{H_2O}		Volume of water[2] (mL/g reaction mass)	Q_{H_2O}		Initiator content[3] (wt %)	Q_{H_2O}	
	25°C	45°C		25°C	45°C		25°C	45°C
0.06	218.1^{g}	232.23^{f}	1.6	63.74^{f}	67.78^{f}	0.32	316.83^{c}	318.8^{c}
0.12	282.8^{d}	323.52^{b}	3.2	185.60 ^{e}	187.60^{e}	0.64	344.30^{b}	447.333^{a}
0.20	316.66^{c}	370.23^{a}	4.8	279.80^{c,d}	325.13^{b}	0.96	228.65^{e}	265.917^{d}
0.25	210.96^{h}	250.53^{e}	6.4	288.23^{c}	376.70^{a}	1.90	213.83^{f}	231.533^{e}
0.30	149.60^{j}	189.00^{i}	8.0	190.67^{e}	265.56^{d}			
0.75	115.16^{k}	151.27^{j}						
1.5	76.36^{l}	77.30^{l}						
LSD at 5%	5.70			16.14			10.86	

Means within a column followed by different letters are significantly different at 5% level of significance and those followed by the same letter do not differ significantly at 5% level of significance.

[1] Synthesis parameters: weight ratio of monomer, clay, and initiator to backbone: 2 : 1, 0.1 : 1, and 0.04 : 1, respectively. V_{H2O} 4.8 mL/g feed.

[2] Synthesis parameters: weight ratio of monomer, clay, cross-linker, and initiator to backbone: 2 : 1, 0.1 : 1, 0.006 : 1, and 0.04 : 1, respectively.

[3] Synthesis parameters: weight ratio of monomer, clay, and cross-linker to backbone: 2 : 1, 0.1 : 1, 0.006 : 1, and 0.04 : 1, respectively. V_{H2O} 4.8 mL/g feed.

TABLE V
Effect of Particle Size of Back Bone Polymer on the Water Absorbency

Particle size (mesh)	Q_{H_2O} (g/g) 25°C	Q_{H_2O} (g/g) 45°C
10.0–25.0	>302.39^g	>376.06^e
25.0–100.0	>313.20^f	>390.00^d
100.0–240.0	>438.53^b	>450.50^a
<240.0	>405.03^c	>409.66^c

LSD at 5%: 9.53; Means within columns followed by different letters are significantly different at 5% level of significance and those followed by the same letter do not differ significantly at 5% level of significance.

Effect of particle size of backbone polymer on the water absorbency

The effect of backbone particle size on Q_{H_2O} values is shown in Table V. It can be seen that decrease in particle size up to 100–240 mesh size resulted in significant increase in the swelling ratio at both 25°C and 45°C. Subsequent decrease, however, exhibited fall in absorbency. This may be explained in terms of increase in specific surface area of backbone with decrease in particle size, leading to its superior expansion and swelling in aqueous medium that seemed to form a network structure of optimum cross-link density. Composite prepared with particle size <240 mesh size exhibited decrease probably because of inability of initiator to generate sufficient free radicals on the highly expanded backbone chains, resulting in low cross-link density.

Absorbency rate measurements

Absorption rates of NSAPC and P-gel were compared in distilled water at three different temperatures. The results shown in Figure 3 indicate that both the gels exhibit sensitivity toward change in temperature as Q_{H_2O} increased with temperature increase from 25°C to 45°C. Rates of absorption, however, varied in the two gels. Except at 25°C, NSAPC attained maximum absorption in 8 h at 35°C and 45°C, whereas the P-gel attained the same in 12 h irrespective of temperature. Buchanan et al.[40] suggested that the swelling kinetics for an absorbent is a function of swelling capacity, particle size distribution of the powder, and specific surface area of the polymer. Introduction of clay into the gel matrix of NSAPC resulted not only in enhancement of the absorption rate, but also increase in the Q_{H_2O} value compared with that of P-gel. This is primarily because of the ability of OH groups of clay to bind water, resulting in formation of a rapid microstream of water.

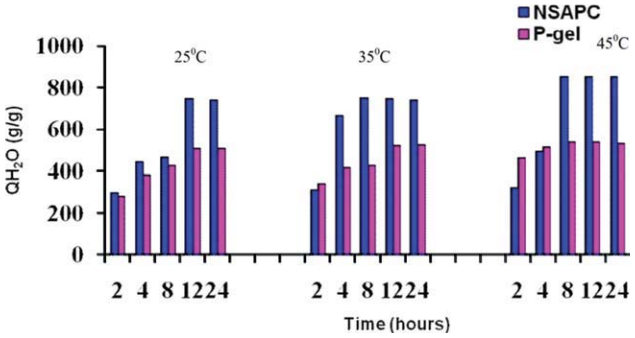

Figure 3 Absorption rate of NSAPC and P-gel in distilled water. [Color figure can be viewed in the online issue, which is available at wileyonlinelibrary.com.]

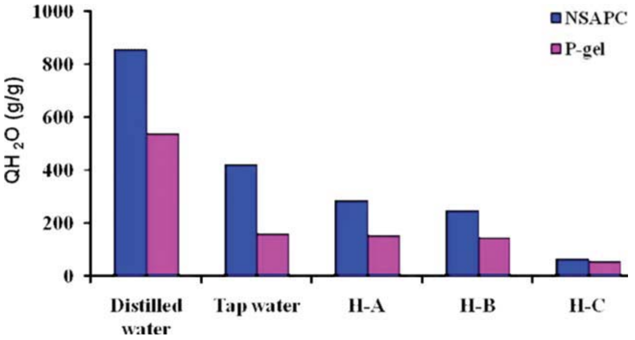

Figure 4 Water absorbency of NSAPC and P-gel as a function of water quality. H-A, H-B, and H-C denote hard water of strengths 20, 326, and 500 ppm, respectively. [Color figure can be viewed in the online issue, which is available at wileyonlinelibrary.com.]

Effect of quality of water on absorbency

Water quality plays an important role in performance of superabsorbents in agriculture. The effect of water quality on the swelling ratio of NSAPC and P-gel is shown in Figure 4. Compared with distilled water, the absorbency values are less in both the polymers. However, water uptake of NSAPC was significantly higher relative to P-gel in all water types. In hard water, the Q_{H_2O} decreased with increase in ionic strength. The decrease may be attributed to screening of anions by the cations in the hard water, which increased with the strength. Also, increase in divalent Ca and Mg ions resulted in increase in degree of cross-linking and the consequent fall in absorbency. This observation is supported by earlier work by Pourjavadi et al. in 2008.[41]

Effect of pH on water absorbency

As shown in Figure 5, swelling capacity of both the "ionic hydrogels" was maximum at pH 7.0. Under acidic pH, swelling is significantly reduced, primarily because of protonation of most of the $-COO^-$ groups, which, in turn, resulted in elimination of repulsive forces among anions. Increasing the pH of

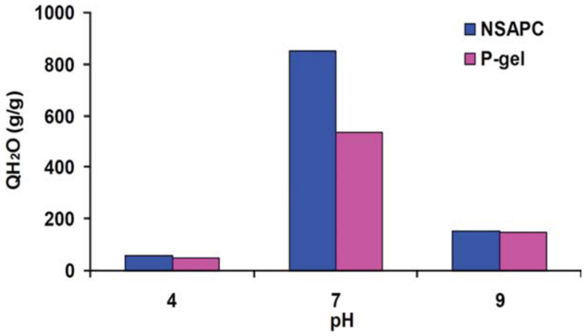

Figure 5 Water absorbency of NSAPC and P-gel as a function of pH of solutions. [Color figure can be viewed in the online issue, which is available at wileyonlinelibrary.com.]

solution from 7 to 9 also resulted in fall in water absorbency values. Swelling loss in highly basic solutions is attributed to the charge screening effect of excess Na^+ on the carboxylate anions, preventing expansion and swelling of the network.

Effect of salt type and strength on water absorbency

Evaluation of the swelling behavior of superabsorbent composites in various types of salt solutions, particularly those applied as fertilizers and present in saline soils, is very important in view of their agricultural and horticultural applications. Figure 6 depicts the comparative swelling of the optimized composite NSAPC and the commercialized gel, P-gel, in solutions of varying strengths of $(NH_4)_2SO_4$, NH_4NO_3, KNO_3, NaCl, and urea. In all the salt solutions, absorption was lesser compared with that in distilled water. Both the gels exhibited minimum decrease in urea solution at all concentrations. This observation bears significance because for most of the crops in agriculture, urea comprises an important fertilizer in tropics and test hydrogels can be recommended for simultaneous application with basal dose of urea. P-gel exhibited relatively more absorption in all the salt types. In general, water absorption decreased with the increase in concentration of salt solution, irrespective of the type of the salt and gel type.

The result may be attributed to the reduction in osmotic pressure difference between gel matrix and external salt solution with increasing ionic strength. For a given salt, the absorbency pattern was flatter in NSAPC (composite) compared with P-gel (clay-free). This observation is in contrast with the observation by Li et al.,[42] who reported that with increasing clay content, the % reduction in absorbency in a salt solution decreased. It can be explained in terms of difference in the nature of backbone in two gels. Inherent presence of -COOH groups in the structure of backbone in the composite may have led to relatively higher extent of screening by salt cations.

The effect of ionic strength on water absorption can be understood in terms of following equation by Hermans:[43]

$$Q_{eq}^{5/3} = A + Bi^2/I$$

where Q_{eq} is the water absorbency at equilibrium, i is the concentration of charges bound to the gel, I is the ionic strength of the external solution, and A and B are the empirical parameters. As seen in Figure 6, for higher ionic strengths, linear relationship between ${Q_{eq}}^{5/3}$ and $1/I$ were observed. This corresponded to counteraction of swelling force by cross-linked network's elastic force.[35]

Effect on water absorption and retention capacity of sandy loam soil and soil-less medium

Water absorption by gel-amended soil and soil-less media showed significantly higher degrees of moisture contents compared with control (Fig. 7). NSAPC-amended soil absorbed more water at both

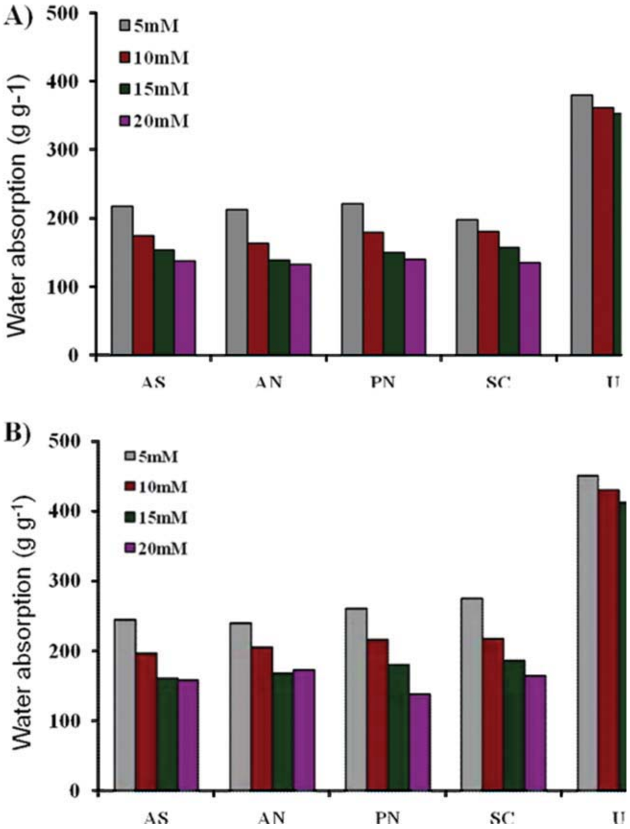

Figure 6 Effect of different salt solutions with varying ionic strength on water absorbency of (A) NSAPC (composite) and (B) P-gel. AS, $(NH_4)_2SO_4$; AN, NH_4NO_3; PN, KNO_3; SC, NaCl; and U, urea. [Color figure can be viewed in the online issue, which is available at wileyonlinelibrary.com.]

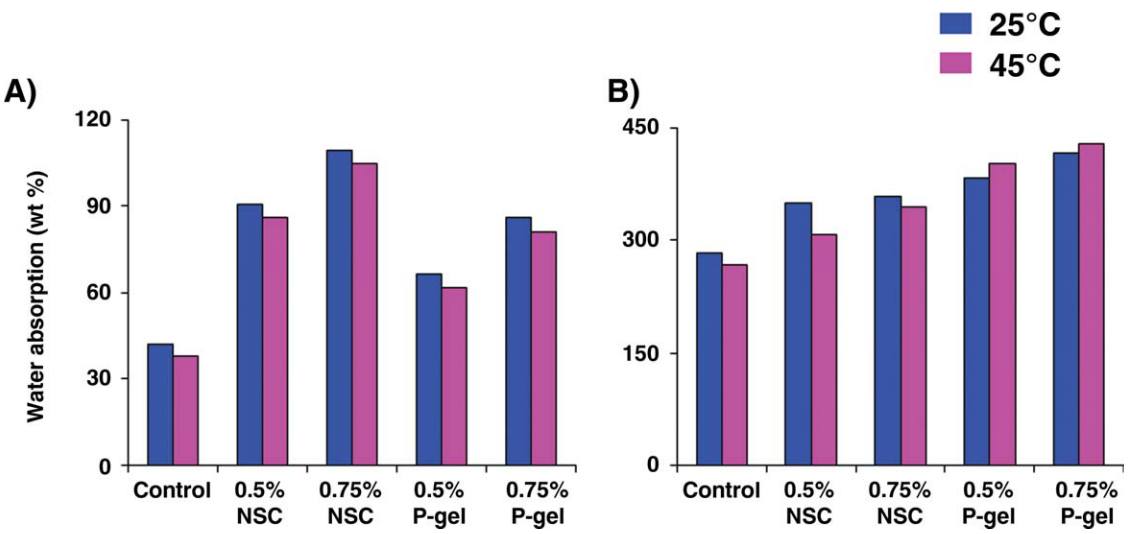

Figure 7 Water absorption capacity of (A) soil and (B) soil-less media as a function of NSAPC and P-gel. [Color figure can be viewed in the online issue, which is available at wileyonlinelibrary.com.]

25°C and 45°C relative to P-gel-amended soil. In soil-less medium, however, reverse behavior was observed. P-gel-amended medium absorbed more water than the NSAPC-amended medium. In soil, amendment with either gel at 0.75% exhibited significantly higher absorbency values compared with 0.5% application rate. On the other hand, in soil-less medium, amendment at 0.5% and 0.75% in each gel led to almost similar degree of absorption, indicating that for nursery raising practices using soil-less medium, amendment at 0.5% gel on weight basis is sufficient.

The above part of study brought out the fact that irrespective of the type of absorbent material, % moisture absorbed by free absorbent was more than when it is present in the plant growth medium. This is because in the amendment, the gel particle is surrounded by soil or media particles, which subject it to confining pressure,[44] limiting the degree of its swelling.

Utility of a superabsorbent material for agricultural and horticultural applications is evaluated in

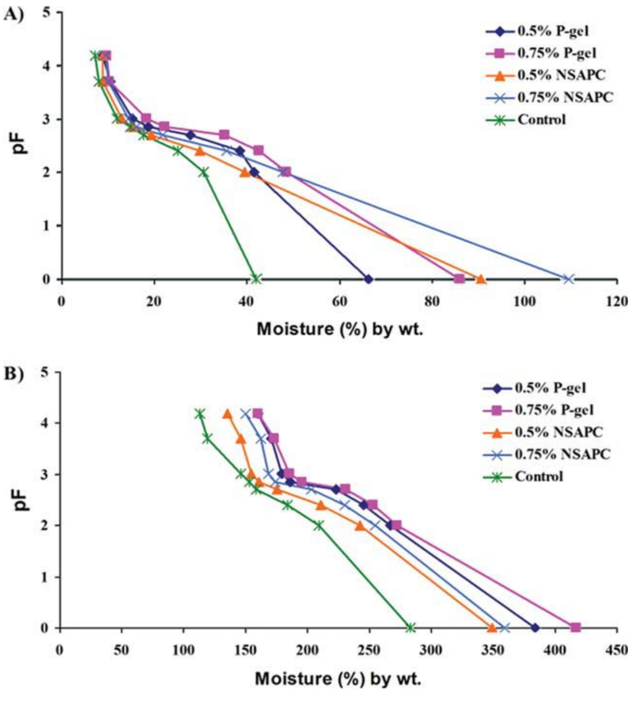

Figure 8 Moisture retention curves of soil (A) and soil-less media (B) under different matric tensions (pF) in control and amended condition. [Color figure can be viewed in the online issue, which is available at wileyonline library.com.]

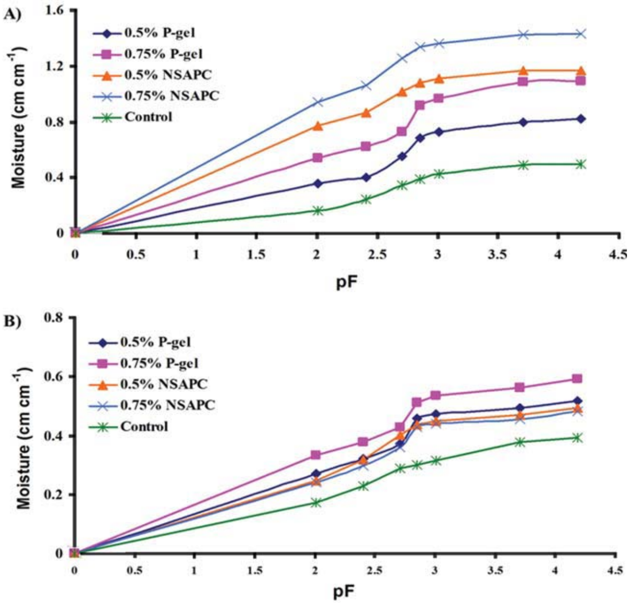

Figure 9 Moisture release curves of soil (A) and soil-less media (B) amended with P-gel and NSAPC. [Color figure can be viewed in the online issue, which is available at wileyonlinelibrary.com.]

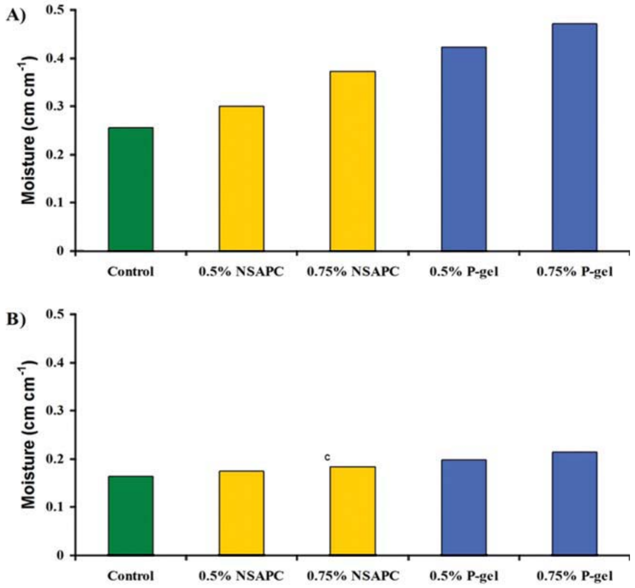

Figure 10 Effect of gel addition on available water from soil (A) and soil-less media (B). [Color figure can be viewed in the online issue, which is available at wileyonlinelibrary.com.]

terms of its moisture characteristics under tension. High and positive correlations were found between soil water content and matric tension using potential functions (Fig. 8). Compared with control, WHC of soil and soil-less media amended with both the test gels remained higher with rise in matric tension. At field capacity (2.53pF), % water content retained in P-gel-amended soil was higher than the NSAPC-amended soil, whereas in case of soil-less medium, almost equal amount of water was retained in both the gels, particularly when applied at 0.75% rate.

Moisture release curve (Fig. 9, expressed in terms of difference in moisture held at zero pressure and at a particular pressure) indicates that soil amendment with 0.75% NSAPC led to maximum improvement in its water release property. As expected, 0.75% P-gel-amended soil-less medium exhibited the most superior moisture release pattern.

The effect of gel addition on the water availability behavior of soil and soil-less medium is shown in Figure 10. Readily available water refers to difference in field capacity and soil moisture at a threshold value of matric tension that provokes plant water stress. Available water in amended soil and soil-less media was calculated from the following expression:[45]

$$\text{Available Water Capacity (AWC)} = (\text{FC} - \text{PWP})\rho_b/100$$

where, FC is percent moisture content in the root zone on weight basis at field capacity level (2.53pF), PWP is percent moisture content on weight basis at wilting point (4.20pF), and ρ_b is bulk density (g cm^{-1}) of soil/medium.

Addition of test hydrogels to soil and soil-less media significantly increased the availability of water to plant compared with control. In case of soil-less medium, the lower rate of application (0.5%) was as effective as higher rate (0.75%) for both the gels. This observation was substantiated by the values of onset wilting point in amended and unamended plant growth media (Fig. 11). As is clear, because of more availability of water in gel-amended treatments, the permanent wilting point approached in the amended soil in 4.7–6.3 days compared with 2.4 days in control. Delay by 1.4–3.6 days was observed in soil-less media.

CONCLUSIONS

Effects of synthesis parameters on the swelling characteristics of a series of novel polyacrylate graft biopolymer clay-intercalated nanocomposites were studied. The study showed that clay/backbone ratio, monomer concentration, cross-linker concentration, and quantity of water per unit reaction were critical parameters in determining the swelling properties of composites. Characterization by XRD confirmed the formation of nanocomposites. Scanning electron microscopy analysis showed polymer–clay interaction and participation

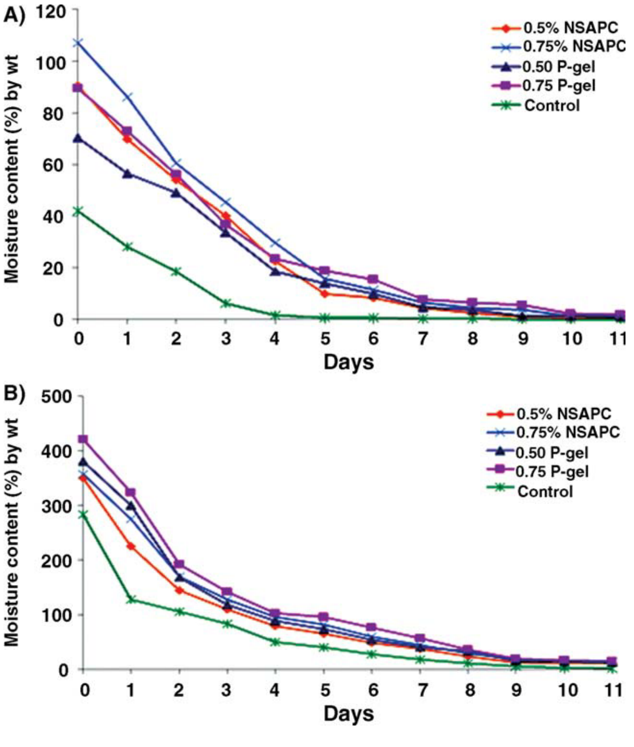

Figure 11 Effect of hydrogel concentration on water storage of sandy loam soil (A) and soil-less media (B). [Color figure can be viewed in the online issue, which is available at wileyonlinelibrary.com.]

of clay in the reaction. The effect of temperature, pH, and salinity on swelling behavior was investigated. Drastic fall in water absorption capacity was not observed in the presence of urea, a major nitrogenous fertilizer used in tropics. Water absorbency and retention behavior of the optimized composite studied under simulated conditions in soil and soil-less medium as applicable in agriculture and horticulture and compared with commercially available product P-gel were found to be significantly higher than the control and comparable with P-gel under most of the conditions. The findings on effect of addition of nanocomposite on the moisture absorption, retention, release, and availability characteristics of plant growth media indicate toward its scope in enhancing water use efficiency in conservation agriculture.

References

1. Hedrick, R. M.; Mowry, D. T. Soil Sci 1952, 73, 427.
2. El-Handy, O. A.; Abo-Sedera S. A. Int J Agri Biol 2006, 8, 876.
3. Bhardwaj, A. K.; Shaiberg, I.; Goldstein, D.; Warrington, D. N.; Levy, G. J Soil Sci Soc Am J 2007, 71, 406.
4. Johnson, M. S.; Leah, R. J Sci Food Agric 1990, 52, 413.
5. Johnson, M. S. J Sci Food Agric 1984, 35, 1063.
6. Chauhan, G. S.; Mahajan, S. J Appl Polym Sci 2002, 86, 667.
7. Rudzinski, W. E.; Dave, A. M.; Viashnav, U. H.; Kumbar, S. G.; Kulkarni, A. R. Aminabhavi, M. Des Monomers Polym 2002, 5, 39.
8. Aminabhavi, T. M.; Kulkarni, A. R.; Soppimath, K. S.; Dave, A. M.; Mehta, M. H. J Appl Polym Sci 1999, 73, 2437.
9. Dave, A. M.; Mehta, M. H.; Aminabhavi, T. M.; Kulkarni, A. R.; Soppimath, K. S. J Polym Plast Technol Eng 1999, 38, 673.
10. Kumbar, S. G.; Kulkarni, A. R.; Dave, A. M.; Aminabhavi, T. M. J Appl Polym Sci 2001, 82, 2863.
11. Kumbar, S. G.; Aminabhavi, T. M. J Appl Polym Sci 2002, 84, 552.
12. Taylor, K. C.; Halfacre, R. G. Hort Sci 1986, 21, 1159.
13. Wang, Y. T.; Gregg, L. L. J Am Soc Hort Sci 1990, 115, 943.
14. Elliott, G. C. J Am Soc Hort Sci 1992, 117, 757.
15. Blodgett, A. M.; Beattie, D. J.; White, J. W.; Elliott, G. C. Hort Sci 1993, 28, 633.
16. Fonteno, W. C.; Bilderback, T. E. J Am Soc Hort Sci 1993, 118, 217.
17. Davies, F. T.; Castro-Jimenez, Y. Sci Hort 1989, 41, 97.
18. Wang, Y. T.; Boogher, C. A. J Rio Grande Valley Hort Soc 1989, 42, 51.
19. Bres, W.; Weston, L. A. Hort Sci 1993, 28, 1005.
20. Martinz, F. X.; Contreras, F.; Lopez, N. Acta Hort 2000, 554, 59.
21. Ahmad, M.; Verplancke, H. Pakistan J Forest 1994, 44, 53.
22. Wallace, G. P. Hort Sci 1988, 23, 998.
23. Henderson, J. C.; Hensley, D. L. Hort Sci 1985, 20, 667.
24. Ingram, D. L.; Yeager, T. H. J Environ Hort 1987, 5, 19.
25. Wang, Y. T.; Boogher, C. A. J Environ Hort 1987, 5, 127.
26. Wang, Y. T.; Gregg, L. L. J Am Soc Hort Sci 1990, 115, 943.
27. Falatah, A. M.; Choudhary, M. I.; Al-Omran, A. M. Arid Soil Res Rehabil 1996, 10, 277.
28. Anupama; Kumar, R.; Parmar, B. S. Indian Pat. Appl. 3462/DEL/2005.
29. Falatah, A. M.; Al-Omran, A. M. Arid Soil Res Rehabil 1995, 9, 91.
30. William, G. E.; Aldo, B. A.; Jinwen, Z. Maderas Ciencia Technologia 2005, 7, 159.
31. Park, H.; Lee, W.; Park, C.; Cho, W.; Ha, C. J Mater Sci 2003, 38, 909.
32. Hule, R. A.; Pochan, D. J. MRS Bull 2007, 32, 354.
33. Anupama; Sarkar, D. J.; Parmar, B. S. Indian Pat. Appl. 1292/DEL/2010.
34. Grim R. E. Clay Mineralogy, 2nd ed.; McGraw-Hill, Inc.: New York, 1968.
35. Reyes, Z.; Clark, C. F.; Comas, M.; Russell, C. R.; Rist, C. E. Nucl Appl 1969, 6, 509.
36. Wu, J.; Wei, Y.; Lin, J.; Lin, S. Polymer 2003, 44, 6513.
37. Flory, P. J. Principles of Polymer Chemistry; Cornell University Press: Ithaca, NY, 1953.
38. Chen, J. W.; Zhao, Y. M. J Appl Polym Sci 1999, 74, 119.
39. Zhou, W. J.; Yao, K. J.; Kurth, M. J. J Appl Polym Sci 1996, 62, 911.
40. Buchanan, K. J.; Hird, B.; Letcher, T. M. Polym Bull 1986, 15, 325.
41. Pourjavadi, A.; Farhadpour, B.; Seidi, F. Starch/Stärke 2008, 60, 457.
42. Li, A.; Wang, A.; Chen, J. J Appl Polym Sci 2004, 94, 1869.
43. Hermans, J. J. Flow Properties of Disperse System; Wiley-InterScience: New York, 1953; p 61.
44. Buchholz, F. L. In Absorbent Polymer Technology; Brannon-Peppas, L., Harland, R. S., Eds.; Elsevier Science: New York, 1990; pp 23–44.
45. Singh, A. K.; Singh, S.; Nathan, K. K.; Chinnusamy, V. A. Practical Manual on Soil-Water-Plant-Environment System; Water Technology Centre, IARI: New Delhi, India, 2004.